

Supporting Information for

“Radial nanowire light-emitting diodes in the
 $(\text{Al}_x\text{Ga}_{1-x})_y\text{In}_{1-y}\text{P}$ material system”

*Alexander Berg,[†] Sadegh Yazdi,^{‡,⊥} Ali Nowzari,[†] Kristian Storm,[†] Vishal Jain,^{†,§}
Neimantas Vainorius,[†] Lars Samuelson,[†] Jakob B. Wagner,[‡] Magnus T. Borgström^{†,*}*

[†]Solid State Physics and NanoLund, Lund University, Box 118, SE-221 00, Lund,
Sweden

[‡]Center for Electron Nanoscopy, Technical University of Denmark, DK 2800 Kgs.
Lyngby, Denmark

[§]Laboratory of Mathematics, Physics and Electrical Engineering, Halmstad University,
Box 823, SE-301 18 Halmstad, Sweden

[⊥]Present Address: Department of Materials Science and NanoEngineering, Rice
University, 6100 Main Street MS-325, Houston, TX 77005, United States

layer	χ_{TMAI}	χ_{TMG}	χ_{TESn}	χ_{H2S}
p-GaInP	-	3.812×10^{-5}	-	-
p-AlGaInP	1.803×10^{-5}	2.965×10^{-5}	-	-
i-GaInP	-	3.812×10^{-5}	-	-
n-AlGaInP:Sn	1.442×10^{-5}	2.372×10^{-5}	8.5×10^{-7}	-
n-AlGaInP:S	1.803×10^{-5}	2.965×10^{-5}	-	2.56×10^{-6}
n-GaInP:Sn	-	3.389×10^{-5}	8.76×10^{-6}	-
n-GaInP:S	-	3.812×10^{-5}	-	1.385×10^{-5}

Table S1. Molar fractions of the precursors for lattice-matched radial GaInP and AlGaInP NW shells for material compositions close to intended $\text{Ga}_{0.47}\text{In}_{0.53}\text{P}$ and $(\text{Al}_x\text{Ga}_{1-x})_{0.47}\text{In}_{0.53}\text{P}$, respectively (Figure 3). For p- and n-AlGaInP the values for the lowest χ_{TMAI} (out of five different runs, Table S2) are displayed. $\chi_{\text{TMI}} = 3.509 \times 10^{-5}$, $\chi_{\text{PH3}} = 1.54 \times 10^{-2}$ and $\chi_{\text{DEZn}} = 3.13 \times 10^{-6}$ were constant during shell growth. The shells were grown at 650 °C.

We varied the $\chi_{\text{TMAI}} / (\chi_{\text{TMAI}} + \chi_{\text{TMG}})$ ratio during growth of the p- and n-AlGaInP layers to find out the relation between the precursor molar fractions and the conduction band offset of the AlGaInP layers. The second data point which is out of the trend might arise from the fact that a cross-section closer to the bottom of the NW than for the other four samples might have been investigated.

$\frac{\chi_{\text{TMAI}}}{\chi_{\text{TMAI}} + \chi_{\text{TMG}}}$	Al content x in p-AlGaInP:Zn	Al content x in n-AlGaInP:S
0.38	0.12	0.13
0.42	0.08	0.07
0.47	0.17	0.17
0.55	0.38	0.36
0.63	0.41	0.37

Table S2. Overview over the Al content x in the p-AlGaInP:Zn and n-AlGaInP:S barrier as a function of the $\chi_{\text{TMAI}} / (\chi_{\text{TMAI}} + \chi_{\text{TMG}})$ ratio. S was used for n-type doping. All other growth parameters were the same as in Table S1. The sum $(\chi_{\text{TMAI}} + \chi_{\text{TMG}})$ was constant for all five growth runs.

For the outermost shell n-GaInP two different dopants were used, TESn and H₂S. Figure S1 shows the influence of the two different dopants on the morphology of the side facets.

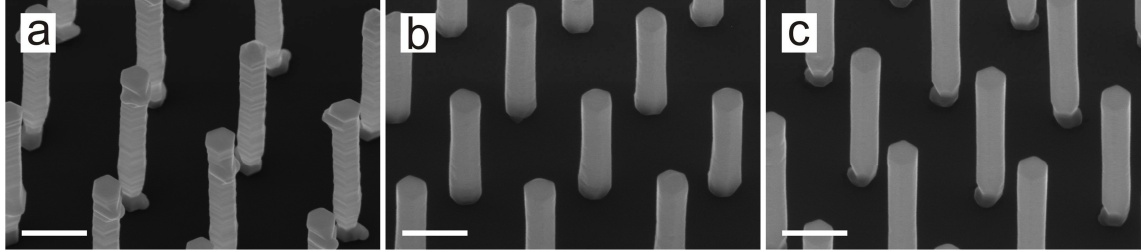


Figure S1. SEM images of the radial GaInP/AlGaInP/GaInP core-shell NWs where (a) Sn ($\chi_{\text{TESn}} = 8.76 \times 10^{-6}$) or (b) S ($\chi_{\text{H}_2\text{S}} = 1.385 \times 10^{-5}$) was used for n-type doping of the outer shell n-GaInP, respectively. In image (c) the outermost shell was intentionally undoped i-GaInP around an n-AlGaInP shell for comparison of the surface morphology. The NWs in images a, b and c have different lengths because their NW cores were grown in different batches. The scale bar is 500 nm. The images were recorded at an angle of 30°.

In order to determine the Al content in the p- and n-AlGaInP NW shell, we performed a series of five growth runs with different $\chi_{\text{TMAI}} / (\chi_{\text{TMAI}} + \chi_{\text{TMG}})$ ratios but with a constant sum $(\chi_{\text{TMAI}} + \chi_{\text{TMG}})$ during growth of the two barriers. Since the Al content cannot be determined by XRD due to the almost same lattice constant of AlP and GaP, we measured it with STEM-EDX.

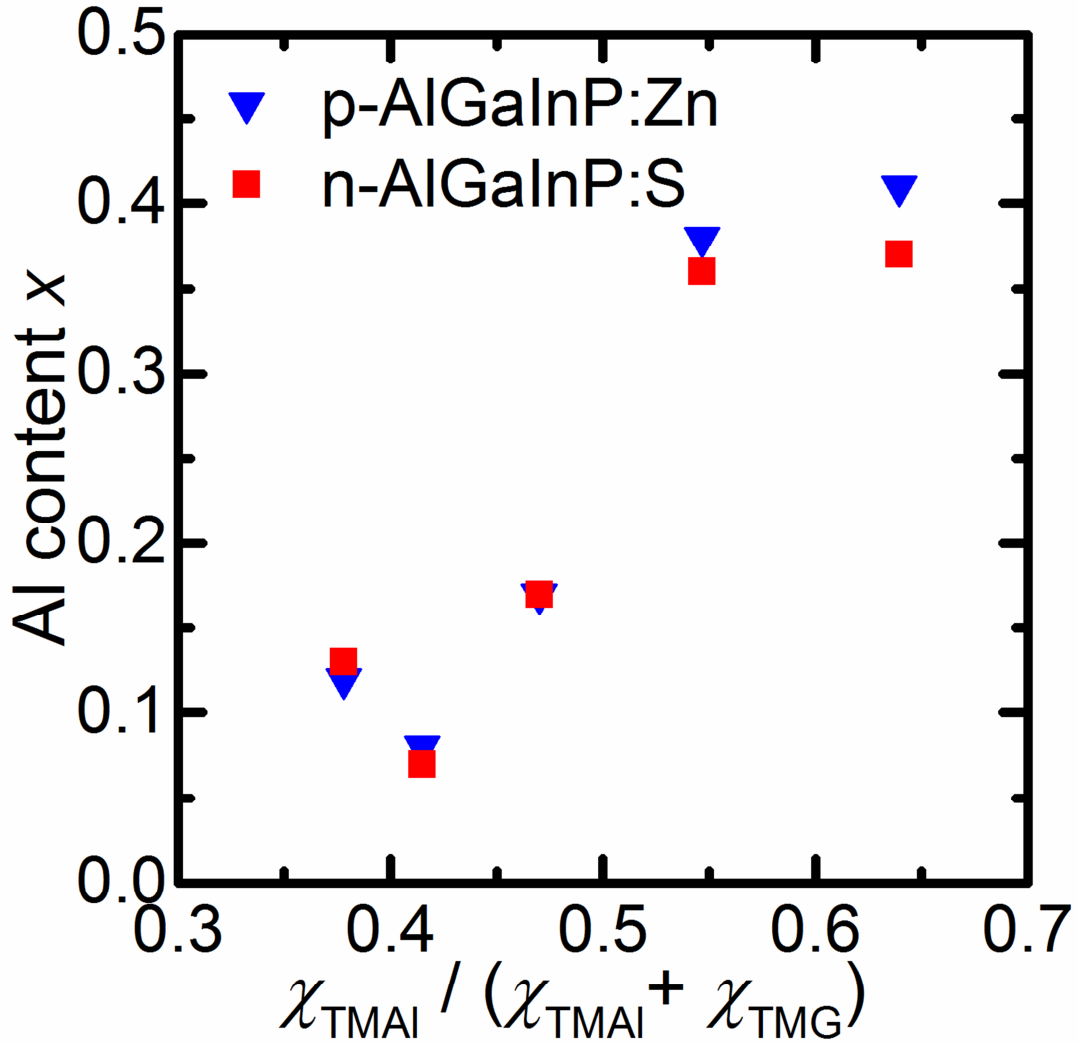


Figure S2. Al content x of the p-AlGaInP:Zn and n-AlGaInP:S barriers in $(\text{Al}_x\text{Ga}_{1-x})\text{InP}$ in radial GaInP/AlGaInP/GaInP core-shell NWs as a function of the precursor molar fractions of TMAI and TMG. The sum $(\chi_{\text{TMAI}} + \chi_{\text{TMG}})$ was constant for all five growth runs in this series. x was determined from the STEM-EDX data.

The optical properties of single NWs of the sample showing the highest IL intensity (10 nm QW thickness) were characterized by photoluminescence (PL) spectroscopy at low temperature (7 K) using a continuous flow liquid helium cryostat. NWs were broken off from the native substrates and spread out on a gold-covered silicon surface. The NW under study was evenly illuminated throughout its length using a frequency doubled yttrium-aluminium-garnet laser. The PL signal was collected by a 20X microscope objective and dispersed onto a thermo-electrically cooled charge coupled device (CCD).

The low temperature PL spectrum has a peak at 1.91 eV and a narrower full-width-at-half-maximum (FWHM) than the respective IL spectrum recorded at room temperature which has its peak at 1.83 eV. The bandgap of GaP and InP at 7 K is 77 and 71 meV higher than at 300 K, respectively, according to the bandgap temperature dependence by Varshni¹ and its parameters A and B by Vurgaftman² and we assume the value for $\text{Ga}_x\text{In}_{1-x}\text{P}$ to lie in between these values.³ We conclude that the PL signal mainly comes from optical transitions within the i-GaInP QW.

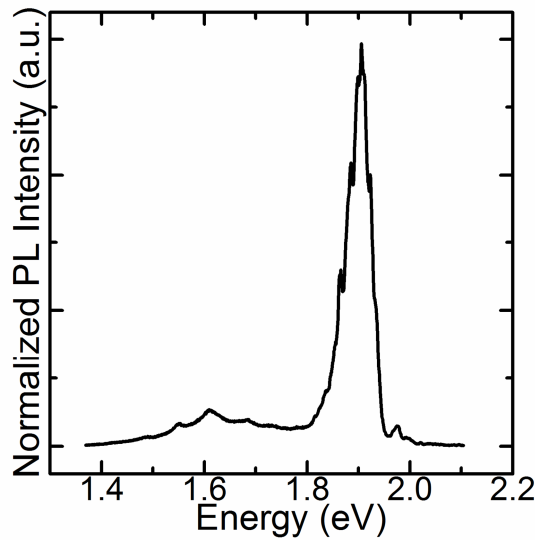


Figure S3. PL spectrum of a single NW with a QW thickness of 10 nm. The NW was grown with the same parameters as the one characterized by injection luminescence (IL).

REFERENCES

1. Varshni, Y. P. *Physica* **1967**, 34, (1), 149-154.
2. Vurgaftman, I.; Meyer, J. R.; Ram-Mohan, L. R. *J. Appl. Phys.* **2001**, 89, (11), 5815-5875.
3. Berg, A.; Lenrick, F.; Vainorius, N.; Beech, J. P.; Wallenberg, L. R.; Borgström, M. T. *Nanotechnology* **2015**, 26, (43), 435601.